Transactions of the **13th International Conference on Structural Mechanics in Reactor Technology** (SMiRT 13), Escola de Engenharia - Universidade Federal do Rio Grande do Sul, Porto Alegre, Brazil, August 13-18, 1995

The PWR lower head under excessive loading - Model experiments and theoretical assessments

Dolensky, B., Krieg, R.
Forschungszentrum Karlsruhe GmbH, Institut für Reaktorsicherheit, Karlsruhe, Germany

ABSTRACT: Several tests with small scale models of a PWR lower head under internal pressure have been carried out up to failure. The results are compared with calculations. The parameter sensitivity of the resulting plastic deformations is discussed.

1. INTRODUCTION

In case of a severe PWR accident the lower head of the reactor pressure vessel may undergo excessive loadings possibly causing structural failure. For instance, the temperature of the lower head may increase, consequently the material strength will decrease, while the system pressure is maintained (core melt-down accident - high pressure path); or the lower head may be loaded dynamically (in-vessel steam explosion). In all of these cases the lower head deformations occuring before failure are of interest.

Therefore, several small scale model tests have been carried out under slowly increasing pressure. The tests have been continued up to failure. One goal was to compare the measured deformations versus pressure with calculated values in order to get some informations about the predictive quality of currant computer codes. Another goal was to get some information about the maximum deformations before failure occurs. It is obvious that these later results must be treated with care. The transfer to the much larger dimensions of a real reactor pressure vessel needs additional considerations.

2. MATERIAL OF THE MODELS

For the models the steel 20MnMoNi55 has been used. The material was a piece of the end section of the cylindrical part of a real reactor pressure vessel. The material data have been determined by tensile tests carried out elsewhere [1]. Using these data the true stress - true strain diagram shown in Fig. 1 has been obtained. For this curve it is assumed that for strains $\varepsilon \geq A_g$ the slope does not change.

Later it turned out that a more accurate determination of the true stress - true strain diagram is necessary also for $\varepsilon > A_g$, where necking occurs. Therefore, additional tensile tests have been carried out yielding the improved diagram shown in Fig. 2, [2]. In order to determine the slope for $\varepsilon > A_g$, the necking diameter versus the tensile elongation was measured. By comparison with finite element calculations of the necking process, where the slope of the diagram was treated as a parameter, that slope was found, for which the necking is simulated best.

3. DIMENSIONS AND MANUFACTORING OF THE MODELS

Basis of the investigation was a PWR lower head of spherical geometry with an inside radius of 2560 mm and a wall thickness of 142 mm. Two models have been manufactored scaled down by 1:50, marked by RDB-1a and RDB-1b. Two additional models are scaled down by 1:100, marked by RDB-2a and RDB-2b. The exact wall thicknesses obtained during the cutting process are listed in Tab. I. The maximum deviations occuring at the axes (poles) are included.

4. PRE-CALCULATIONS

Pre-calculations have been carried out with the finite elemente code ABAQUS [3] using the true stress - true strain diagram of Fig. 1. The discretization of the model, including the lower head, a section of the cylindrical shell and the clamping flange, is shown in Fig. 3. Axisymmetry has been assumed, but the actual dimensions of the models including the deviations mentioned in Tab. I have been considered. For the analyses the internal pressure was varied. The resulting deformations were treated as geometry changes (geometric nonlinearity).

The calculated axial displacements versus the internal pressure are presented in Figs. 5 (a - d).

5. EXPERIMENTS

The test device is shown in Fig. 4. The model is clamped to the base plate equipped with channels for the supply of pressurized oil. The pressure is measured by a pressure transducer allowing for a maximum pressure of 800 bar, accuracy ± 3.2 bar. The model deformations are determined by monitoring the axial displacement of the pole during the test and by detailed measuring of the deformed shape and the reduced wall thickness after the test. The accuracy obtained for the axial displacement is ± 0.005 mm.

Initially, the pressure has been increased by steps of about 20 bar taking about two minutes. The pressure and the axial displacement have been registered immediately after the steps and again after a delay of about one minute, where the oil supply was stopped. During this delay the pressure fell down a little bit while the axial displacement was still increasing. At the end of the delay of one minute the relaxation process ceased.

Later when the oil supply caused only minor pressure changes, the steps have been limited by the axial displacement which was allowed to increase by 0.2 mm. However, now the relaxation process was so fast that the measurements immediately after the steps could not be carried out.

The measured axial displacements versus pressure are described in Fig. 5. Up to the maximum pressures the resulting curves are about the same (for comparison the axial displacements of RDB-2a and RDB-3a must be magnified by the factor two, because of the smaller scale). Up to this point the curves agree also very well with the pre-calculations.

However, the axial displacements where failure occured differ considerably. Consequently, also the maximum reductions of the wall thickness which roughly coincide with the maximum equivalent strains are quite different. For more details see the right hand side columns of Tab. I.

In addition, also the type of failure was quite different. For the models RDB-1a, RDB-2a, and RDB-3a large cracks occured (although the fluid inside the model was almost incompressible). For example, see the crack of RDB-3a in Fig. 6. However, for model RDB-1b (where the maximum axial displacement was about twice as much as for RDB-1a), only a very small crack occured.

Furthermore, the overall deformations of model RDB-1b turned out to be asymmetric as shown in Fig. 7, while the deformations of the other models were roughly axisymmetric.

Tab. I: Wall thicknesses and maximum deformations

	measured wall thickness	deviation at the axis	max. axial displacement	max. reduction of wall thickness
RDB-1a	2.72 mm	+ 0.03 mm	6 mm	25 - 30 %
RDB-1b	2.76 mm	+0.08 mm	13 mm	45 %
RDB-2a	1.26 mm	+ 0.00 mm	11 mm*	40 %
RDB-3a	1.37 mm	+ 0.08 mm	9 mm*	30 %

* values magnified by the factor two to account for the smaller scale.

6. REASON FOR THE ASYMMETRIC DEFORMATION OF MODEL RDB-1b

Due to the cutting process using a lathe the geometric asymmetry of the models can be assumed to be extremely small (asymmetry of the wall thickness might be in the order of 0.1 %). Also the variation of the material properties along the circumference is expected to be relatively small (order of 1 %). This suggests that the plastic deformation process of the lower head might be (close to) a bifurcation problem, where (for small parameter variations) two different equilibrium paths exist, the symmetric deformation path and an asymmetric deformation path.

In order to prove this hypothesis an asymmetric finite element model has been developed where the axis of the inside and outside surface have a small distance e. In the cylindrical part this causes a circumferential deviation of the wall thickness of $\pm$e, in the spherical part this deviation vanishes if one approaches the pole. The model is shown in Fig. 8. Test calculations indicated that for e=0 the results were very close to those obtained with the previous model of Fig. 3. In addition, thorough discussions of the problem suggested that the bifurcation effect might occur only for stress - strain diagrams with very small slopes in the region of large plastic strains. Therefore, the more accurate relation shown in Fig. 2 has been used.

Now calculations with e = 0.01 and 0.1 mm led to the expected asymmetry. The shapes of the deformed head are shown in Fig. 9 and 10 with the pressure as parameter. (The scale for geometry and displacements is the same.)

To provide a quantitative description for the asymmetry of the deformations, the left hand side of the lower head was turned over to the right hand side, as shown in Fig. 11, and the difference d between the displacements of corresponding points marked in the figures were determined. For an initial excentricity e = 0.01 mm and for conditions close to those where the model failed, the deformation excentricity turns out to be d $\approx$ 1.4 mm; for e = 0.1 mm the deformation excentricity is d $\approx$ 10.5 mm. In other words, small imperfections are extensively magnified during the deformation process.

Assuming a linear relation between e and d, an initial excentricity of e $\approx$ 0.03 mm which is about 1 % of the wall thickness would be sufficient to cause the deformation excentricity d $\approx$ 3.7 mm which was measured at the model RDB-1b. As mentioned before the initial excentricity of the model geometry was considerably smaller. So this cannot be the reason for the measured deformation excentricity. However, an initial excentricity of the material data of about 1 %, i.e. a variation of the material data along the circumference of about ±1 % can also explain the experimental finding. Such variations of the material behavior might indeed have occured.

7. CONCLUSIONS

The agreement between the calculated and measured axial displacements versus pressure up to the maximum pressure is quite satisfactory. That means, in this region the mechanical behavior of the lower head can be predicted by computational models, if deviations of a few percent are acceptable.

However, calculation of the maximum axial displacements (maximum strains) was not possible, since necking processes which could have terminated the deformation processes did not occur.

Beyond that, the experiments showed that a well defined deformation state where failure occurs does not even exist. In the different tests the maximum axial displacements varied considerably (more than the factor 2). This is probably due to the fact that necking did not occur. Thus failure was controlled by the maximum strain which the material is able to withstand. This, however, depends strongly on local material conditions such as the size of micro cracks, for instance.

In addition the experiments showed that the resulting deformations may be quite asymmetric, although the initial conditions are approximately symmetric. Extended calculations confirmed that this can be explained by the influence of inevitable variations of the material behavior in the lower head.

REFERENCES

[1] S. Müller, W. Kuhn: Ermittlung von Festigkeits- und Verformungskennwerten des Stahls 20MnMoNi55 von Raumtemperatur bis 900 °C. Internal report 1991.

[2] B. Ritter: On the Load Carrying Capacity of a Pressurized and Externally Cooled Reactor Pressure Vessel. Proc. OECD Workshop on Large Molten Pool Heat Transfer, CEN Grenoble (France) 1994.

[3] ABAQUS, User Manual - Version 4.9, Hibbit, Karlsson & Sorensen Inc., 35 South Angell Street, Providence, R.I., USA.

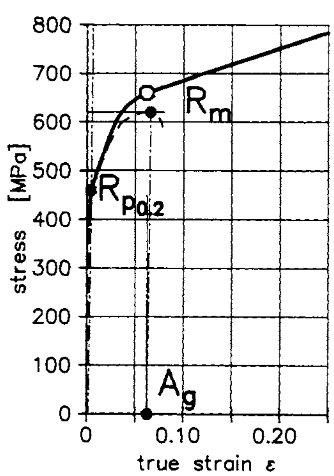

Fig.1: Stress-strain diagram

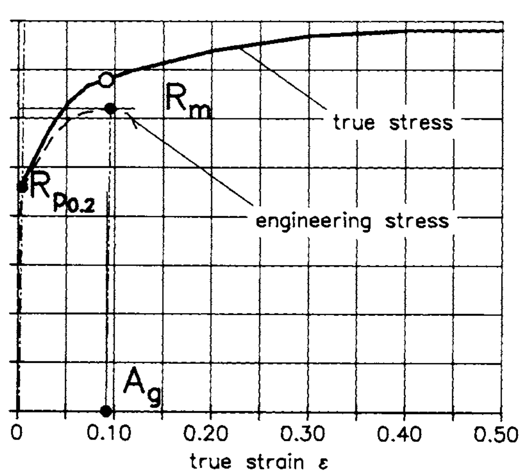

Fig.2: Improved stress-strain diagram

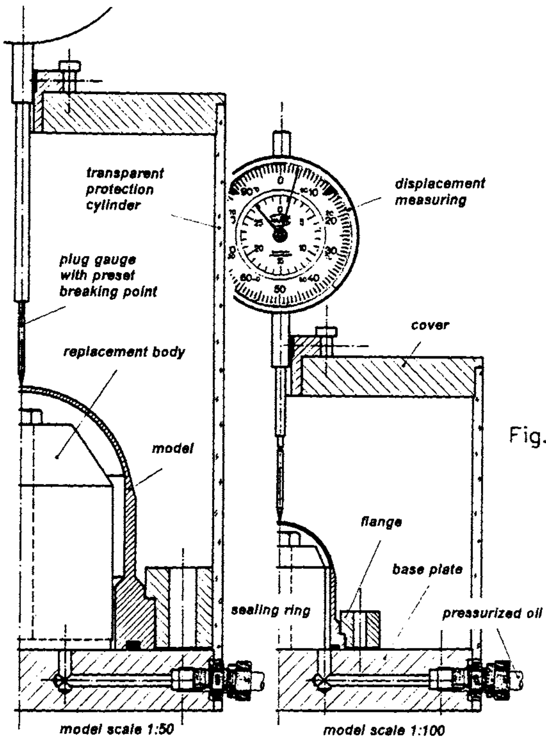

Fig.4: Test device

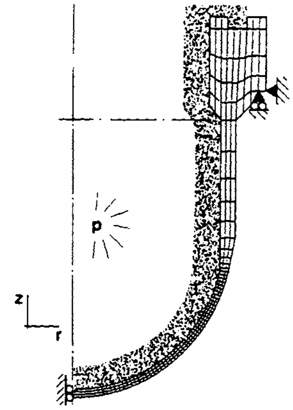

Fig.3: Axisymmetric finite element model

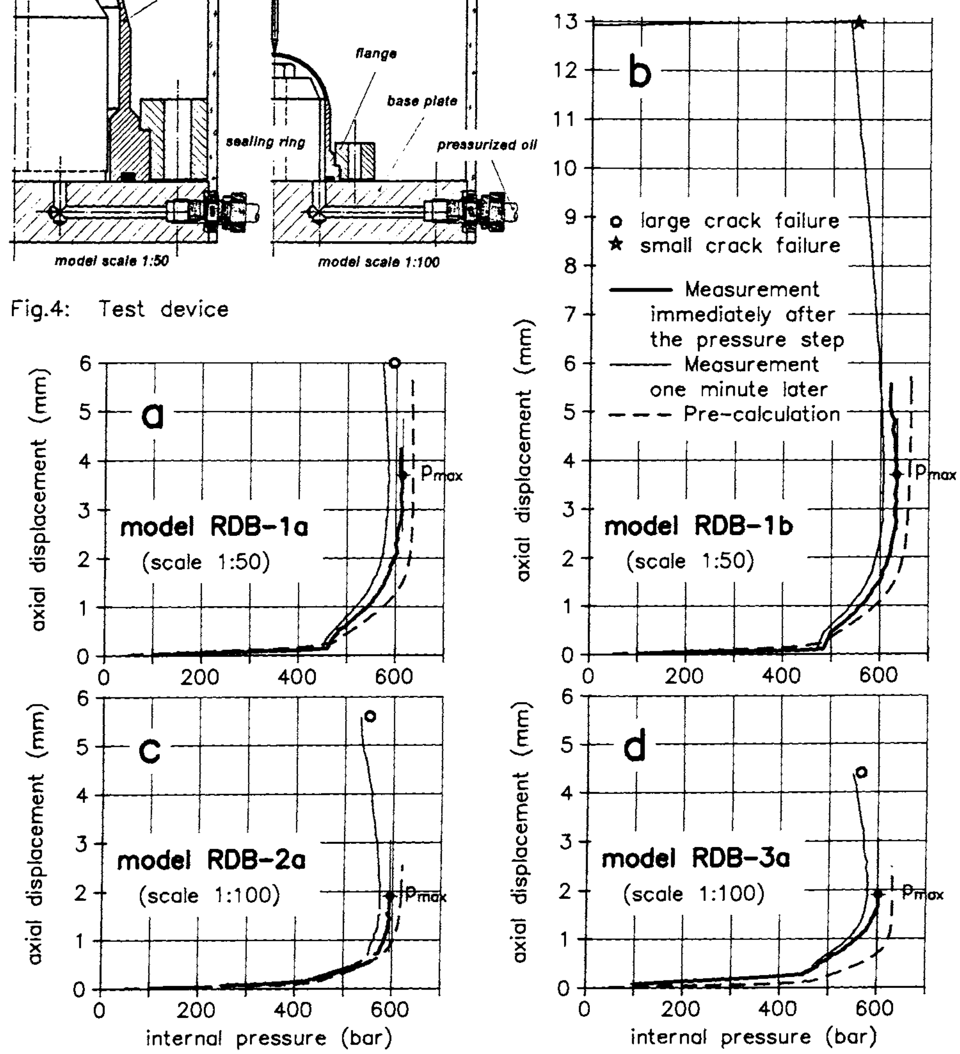

Fig.5(a–d): Axial displacement of the pole versus pressure

Fig.6: Crack in the model RDB-3a

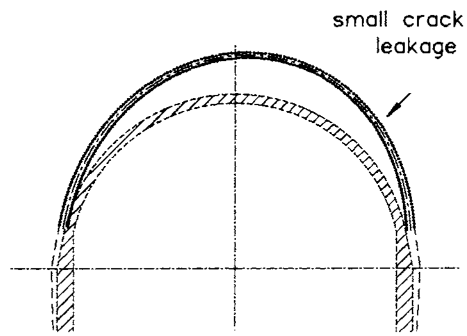

Fig.7: Measured asymmetric deformation of model RDB-1b

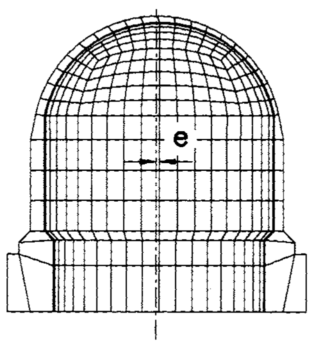

Fig.8: Asymmetric finite element model

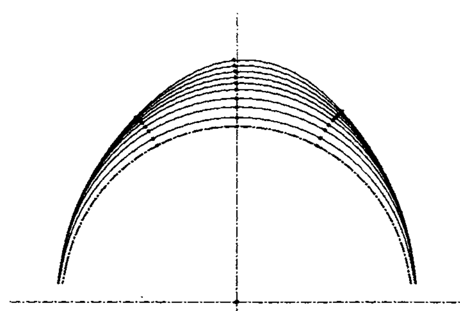

Fig.9: Shape of deformed lower head, initial excentricity e=0.01mm

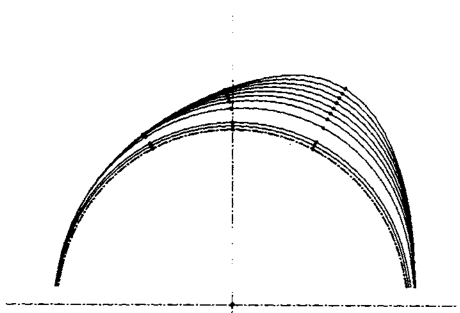

Fig.10: Shape of deformed lower head, initial excentricity e=0.1mm

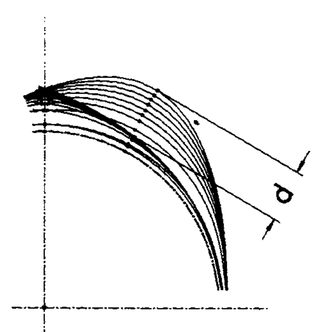

Fig.11: Left hand side turned over to the right hand side, e=0.1mm